The Astrophysical Journal, 903:100 (13pp), 2020 November 10 https://doi.org/10.3847/1538-4357/abbb8e

Blue Large-amplitude Pulsators: The Possible Surviving Companions of Type Ia Supernovae

Xiang-Cun Meng[1,2,3], Zhan-Wen Han[1,2,3], Philipp Podsiadlowski[4], and Jiao Li[1,5]
[1] Yunnan Observatories, Chinese Academy of Sciences, 650216 Kunming, People's Republic of China; xiangcunmeng@ynao.ac.cn
[2] Key Laboratory for the Structure and Evolution of Celestial Objects, Chinese Academy of Sciences, 650216 Kunming, People's Republic of China
[3] Center for Astronomical Mega-Science, Chinese Academy of Sciences, 20A Datun Road, Chaoyang District, Beijing, 100012, People's Republic of China
[4] Department of Astronomy, Oxford University, Oxford, OX1 3RH, UK
[5] Key Laboratory of Space Astronomy and Technology, National Astronomical Observatories, Chinese Academy of Sciences, Beijing 100101, People's Republic of China
Received 2020 August 4; revised 2020 September 9; accepted 2020 September 23; published 2020 November 6

Abstract

The single degenerate (SD) model, one of the leading models for the progenitors of Type Ia supernovae (SNe Ia), predicts that there should be binary companions that survive the supernova explosion, which, in principle, should be detectable in the Galaxy. The discovery of such surviving companions could therefore provide conclusive support for the SD model. Several years ago, a new type of mysterious variable was discovered, the so-called blue large-amplitude pulsators (BLAPs). Here we show that all the properties of BLAPs can be reasonably well reproduced if they are indeed such surviving companions, in contrast to other proposed channels. This suggests that BLAPs could potentially be the long-sought surviving companions of SNe Ia. Our model also predicts a new channel for forming single hot subdwarf stars, consistent with a small group in the present sample of hot subdwarf stars.

Unified Astronomy Thesaurus concepts: Type Ia supernovae (1728); White dwarf stars (1799); Variable stars (1761); Supernova remnants (1667)

1. Introduction

The nature of the progenitors of Type Ia supernovae (SNe Ia) remains a hotly debated topic (Hillebrandt & Niemeyer 2000; Wang & Han 2012; Maoz et al. 2014), even though they have been so important for determining cosmological parameters (Riess et al. 1998; Perlmutter et al. 1999; Meng et al. 2015). At present, a basic framework has been established where an SN Ia originates from the thermonuclear explosion of a carbon–oxygen white dwarf (CO WD) in a binary system (Hoyle & Fowler 1960). The WD accretes material from its companion and increases its mass until close to its maximum stable mass, where a thermonuclear explosion occurs in the WD (Branch 2004). Based on the nature of the companion star of the accreting WD, two classes of progenitor scenarios have been proposed: the single degenerate (SD) model, where the companion is a nondegenerate star, i.e., a main-sequence or a slightly evolved star (WD + MS), a red giant star (WD + RG) or a helium star (WD + He star) (Whelan & Iben 1973; Nomoto et al. 1984), and the double-degenerate (DD) model, involving the merger of two CO WDs (Iben & Tutukov 1984; Webbink 1984). Both models have some support on both the observational and the theoretical sides (Howell 2011).

A basic difference between the two classes of models is that there still is a surviving companion after the supernova explosion in the SD model but not in the DD model (but see Shen et al. 2018). Searching for surviving companions directly in supernova remnants (SNRs) is a viable way to distinguish between the different models. The discovery of potential surviving companions in some supernova remnants has revealed the power of the method (Ruiz-Lapuentec et al. 2004; Li et al. 2017). However, the typical lifetime of an SNR is only a few 10^4 yr (Sarbadhicaryc et al. 2017), which is much shorter than the lifetime of any surviving companion. Therefore, there must be a large number of surviving companions in the Galaxy that are not associated with SNRs, freely cruising in space, if the SD model contributes, at least in part, to the production of SNe Ia. The surviving companion may show some unusual properties compared to normal single stars, e.g., an atmosphere polluted by supernova ejecta and a relative high space velocity (Han 2008). If such surviving companions were discovered, this could provide conclusive support for the SD model.

Recently, Pietrukowicz et al. (2017) found a new class of variable stars named blue large-amplitude pulsators (BLAPs), objects whose origin is still a complete mystery. BLAPs are single, hydrogen-deficient stars associated with the Galactic disk, and no BLAP has been discovered in the Magellanic Clouds (Pietrukowicz 2018); i.e., BLAPs appear to belong to a young population with a relatively high metallicity. Model simulations show that BLAPs are core-helium-burning or shell-hydrogen-burning stars, and that their total mass is smaller than $\sim 1.2\,M_{\odot}$ (Pietrukowicz et al. 2017). Their positions in the Hertzsprung–Russell (H-R) diagram locate them between main-sequence stars and hot sdOB stars, as do their surface gravities; this suggests that the envelopes of BLAPs are slightly more massive than those of hot sdOB stars. However, the lifetime of shell-hydrogen-burning stars during the BLAP stage is too short compared with the lifetime of the BLAPs deduced from the rate of their change in period (Podsiadlowski et al. 2002; Byrne & Jeffery 2018; Córsico et al. 2018; Romero et al. 2018; Wu & Li 2018). This leaves core-helium-burning stars with a thin hydrogen envelope as the only viable solution for BLAPs (Byrne & Jeffery 2018; Wu & Li 2018). To form such a special structure, a star needs to lose its hydrogen-rich envelope after a helium core has formed in its center.

Meng & Podsiadlowski (2017) developed a new version of the SD model, which they named the common-envelope wind (CEW) model. In this model, mass transfer between a WD and

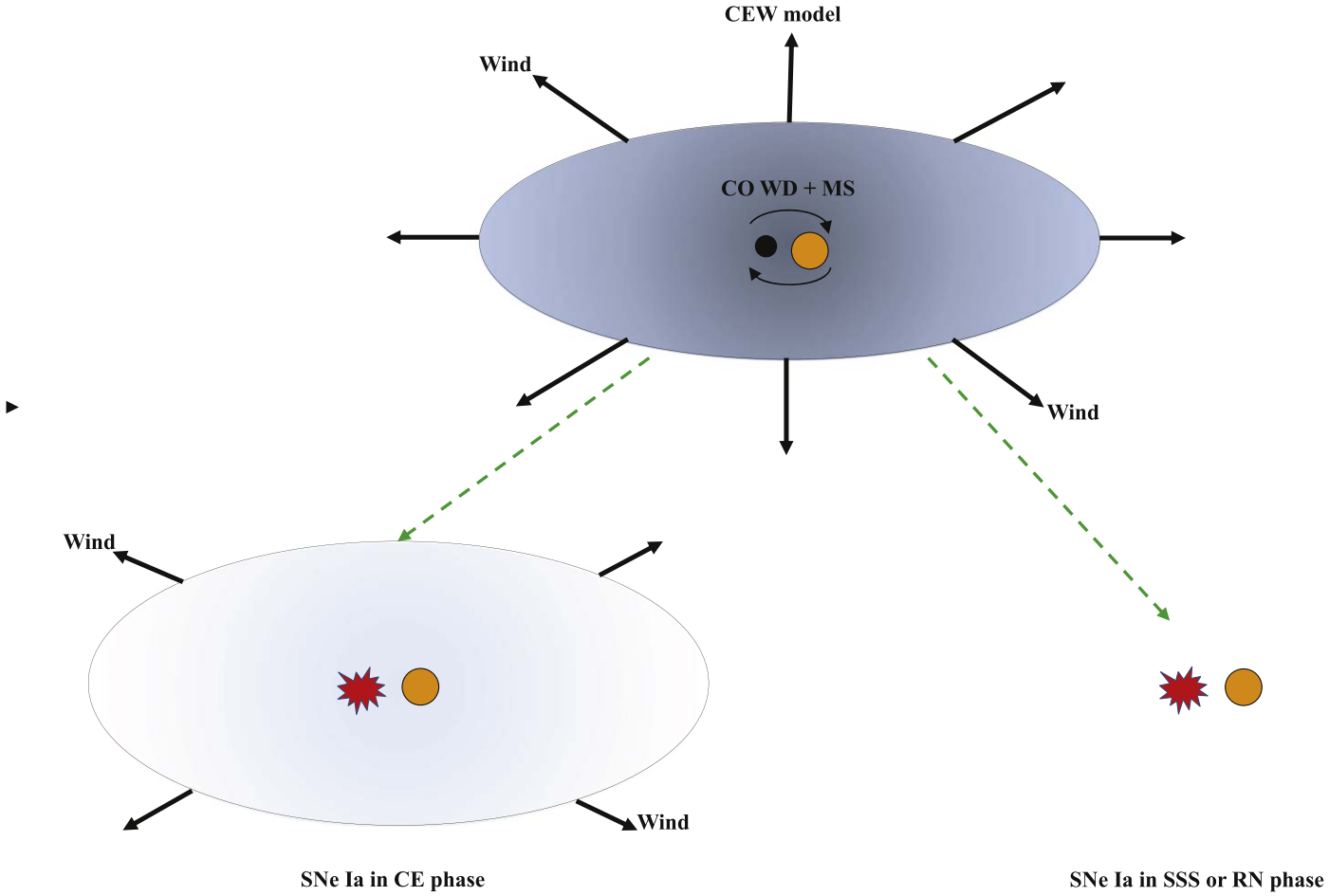

Figure 1. Schematic diagram illustrating the common-envelope wind (CEW) model, where the SN Ia may explode in a CE, SSS, or RN phase. BLAPs originate from those exploding in the CE phase.

its companion can begin when the companion is an MS star or is crossing the Hertzsprung gap (HG). If the mass-transfer rate exceeds the critical accretion rate of the WD, the WD will expand to an RG-like object, and a common envelope (CE) is assumed to form around the binary system. The WD then gradually increases its mass at the base of the CE. For a low density of the CE, the binary system is expected to survive from the CE phase until the WD approaches the Chandrasekhar mass and explodes as an SN Ia. The WD may explode while it is still in the CE phase, a phase of stable hydrogen burning (and appear as a supersoft X-ray sources (SSS)), or in a phase of weakly unstable hydrogen burning, where the system would appear as a recurrent nova (RN), as illustrated in Figure 1. According to the different phases when the SN Ia occurs in the CEW model, even some peculiar SNe Ia may share the same origin: e.g., the so-called SNe Ia-CSM and 02cx-like objects may both originate from the explosions of hybrid carbon–oxygen–neon (CONe) WDs in SD systems (Meng & Podsiadlowski 2018). In the CEW model, if the mass transfer for a binary system begins when the companion crosses the HG, a helium core has been formed in the center of the companion. The core mass is determined by the initial companion mass and the initial orbital period: the more massive the initial companion or the longer the initial orbital period, the more massive the helium core of the companion. After the supernova explosion, such a companion may become a hydrogen-deficient low-mass single star (e.g., Figure 19 in Meng & Podsiadlowski 2017, where the SN Ia explodes in the CE phase) and share many properties with BLAPs, making them promising candidates for surviving companions from SD systems. Here, adopting the CEW model, we will show that all the properties of BLAPs may be simultaneously reproduced by the surviving companions in the CEW model: their population characteristics, their single-star nature, their lifetime as a BLAP, their location in the H-R diagram, their surface helium abundance and surface gravity, their radial velocity, their pulsation periods, including the rate and sign of the change in period, the total number of BLAPs and the number ratio of BLAPs to hot subdwarf stars in the Galaxy. We will also show that there is no other proposed channel that can simultaneously explain all these properties. Hence we suggest that BLAPs are likely surviving companions of SNe Ia, as predicted by the SD model, and that their discovery provides strong evidence in support of the SD model.

In Section 2, we describe our methods and the main results of our calculations. In Section 3 we discuss the results, and we present our main conclusions in Section 4.

2. Methods and Results

2.1. H-R Diagram

In the CEW model, if mass transfer between a relatively massive initial WD and a relatively massive initial companion begins in the HG, the companion can become a hydrogen-deficient, low-mass

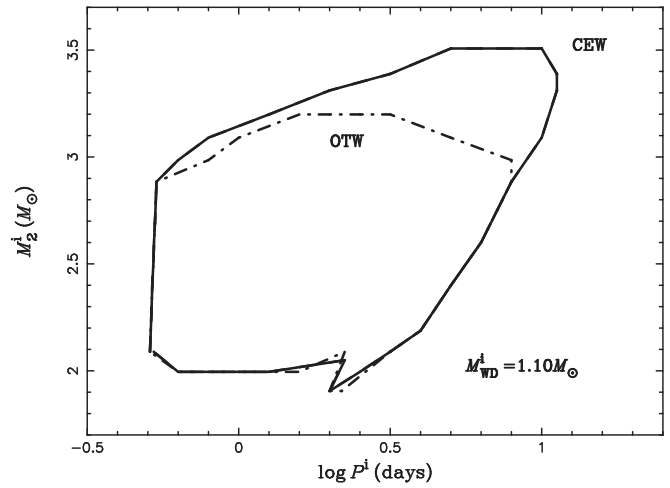

Figure 2. Comparison between the CEW and OTW models for the initial parameter contours leading to SNe Ia, where the initial WD mass is 1.10 $M_\odot$. The data for the plot are taken from Meng et al. (2009) and Meng & Podsiadlowski (2017).

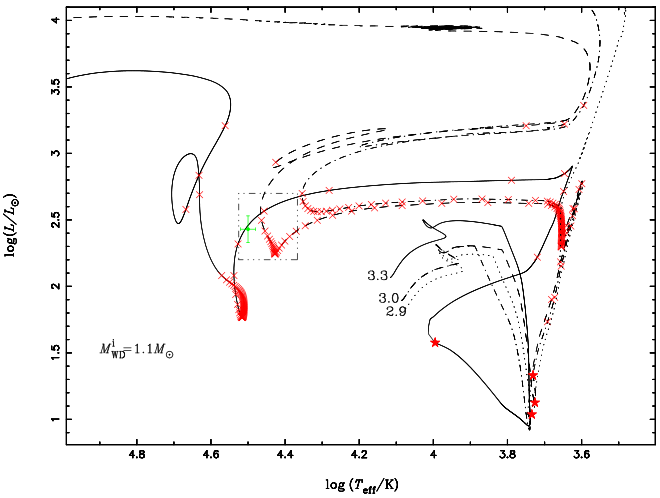

Figure 3. The evolutionary tracks of the companion stars in the H-R diagram. Red stars show the position where the SNe Ia are assumed to occur, and the dashed–triple-dotted rectangle presents the region for BLAPs. The initial WD masses are the same for the four systems, i.e., $M^i_{WD} = 1.1\,M_\odot$. The initial companion masses and periods of the four systems are $[M^i_2/M_\odot, \log(P^i/\mathrm{day})] = (3.3, 0.9)$, $(3.0, 0.8)$, $(3.0, 0.6)$, and $(2.9, 0.7)$, and the evolutionary tracks of the companions from the four systems are shown by solid, dashed, dashed–dotted, and dotted curves, respectively. The age interval between adjacent crosses is 10^6 yr. The green cross represents BLAP-009, whose luminosity is calculated based on the distance from the Gaia DR2 and the average apparent magnitude in Pietrukowicz et al. (2017); the error bar of the luminosity is determined from the distance error in Gaia DR2, and the error bar of the effective temperature comes from the spectral fitting in Pietrukowicz et al. (2017).

single star after the supernova explosion (e.g., Figure 19 in Meng & Podsiadlowski 2017). The surviving companion then has a helium core and a thin hydrogen-rich envelope. If helium is ignited in the core, the star will become a core-helium-burning star with a thin hydrogen-deficient envelope. As far as the companion properties after the supernova explosion are concerned, the difference for most cases between the CEW and the optically thick wind (OTW) model is not very significant (Hachisu et al. 1996; Meng & Podsiadlowski 2017). However, as shown in Meng & Podsiadlowski (2017), some systems that cannot produce SNe Ia in the OTW model may do so in the CEW model (the upper right region in the P_i–M^i_2 plane in Figure 2). Indeed, it is just these systems that are more likely to leave hydrogen-deficient, single-star companions. Considering the merits of the CEW model relative to the OTW model, we here use the CEW model to calculate the evolution of the companion.

We assume that the WDs explode as SNe Ia when $M_{WD} = 1.378\,M_\odot$. Here, we do not consider the effects of spin-up/spin-down and stripping-off on the companions since there are still many uncertainties about how to implement these effects, but we note that they are unlikely to change our basic conclusions (see the discussions in Section. 3.2). After the supernova explosions, the companions may become hydrogen-deficient, single stars, such as BLAPs. To examine whether the surviving companions can reproduce the other properties of BLAPs, we choose four typical binary systems and continue to evolve the companion stars after the supernova explosion and record their various parameters that may be directly compared with the properties of BLAPs.

In Figure 3, we show the evolutionary tracks of the companions in the H-R diagram. Generally, the companions ascend the red giant branch (RGB) after the supernova explosion, and helium is ignited in the core at the tip of the RGB. The companions then become horizontal branch (HB) stars and stay on the HB, while shell hydrogen burning above the helium-burning core continues to consume hydrogen-rich envelope material. However, depending on the different envelope masses of the companions on the HB, their subsequent evolution can become quite different. If the envelope of the companion is so thick that it cannot be consumed completely before the exhaustion of the helium in the center, the star will evolve like a typical asymptotic giant branch (AGB) star (dotted line). In contrast, if the envelope is so thin that it is exhausted soon after helium ignition, the evolutionary track of the companion is similar to that of a hot subdwarf star (solid line, Han et al. 2002, 2003). For the companion from the system with initial parameters of $[M^i_{WD}/M_\odot,\ M^i_2/M_\odot,\ \log(P^i/\mathrm{day})] = (1.1,\ 3.0,\ 0.8)$, the envelope is neither very thin nor very thick. As the envelope is consumed due to shell hydrogen burning on the HB, it becomes thinner and thinner and the effective temperature increases correspondingly. As a result, the evolutionary track of the companion moves to the left and may cross the region where BLAPs are located in the H-R diagram (dashed line). At the BLAP stage, shell hydrogen burning is extinguished, but there is still a very thin hydrogen-deficient envelope left, as has been deduced for BLAPs (Pietrukowicz et al. 2017). Since the companion has spent a long time on the HB, its lifetime in the BLAP stage is shorter than that of a typical hot subdwarf star, but it can still be as long as a few 10^7 yr as inferred for BLAPs (Pietrukowicz et al. 2017). This suggests that BLAPs are in the middle or late phase of helium core burning (see also Wu & Li 2018). In addition, the evolutionary track of the companion from the system with $[M^i_{WD}/M_\odot, M^i_2/M_\odot, \log(P^i/\mathrm{day})] = (1.1, 3.0, 0.6)$ is close to the region of BLAPs, but with a somewhat lower effective temperature because of its thicker envelope.

The different evolutionary tracks of the companions in Figure 3 are therefore mainly due to the different envelope masses at the time of the supernova explosion. BLAPs are hydrogen-deficient, which implies that their progenitors could also be hydrogen-deficient when they are born. Based on the results in Meng & Podsiadlowski (2017), for a system where mass transfer begins when the companion crosses the HG, the

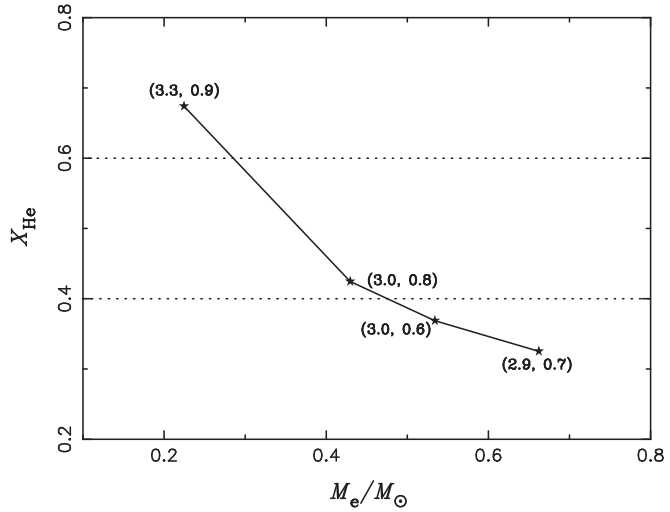

Figure 4. Correlation between the surface helium abundance and the envelope mass of the companion when $M_{\rm WD} = 1.378\,M_{\odot}$ (solid curve), where the four points correspond to the four systems in Figure 3. The dotted curves show the likely regions of the surface helium abundance for BLAPs when $M_{\rm WD} = 1.378\,M_{\odot}$ (see Section 2.3).

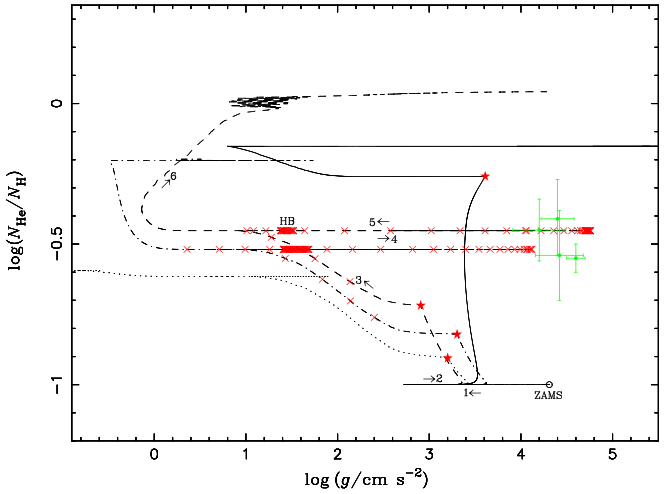

Figure 5. The evolution of the surface helium abundance and gravity of the surviving companions of SNe Ia. The lines represent the same systems as shown in Figure 3, and the red stars show the positions where supernova explosions are assumed to take place. The green crosses represent the four BLAPs with spectroscopic observations in Pietrukowicz et al. (2017), and the age interval between adjacent crosses is 10^6 yr. The arrow and numbers mark the evolutionary direction of the model with $[M^{\rm i}_{\rm WD}/M_{\odot},\ M^{\rm i}_{2}/M_{\odot},\ \log(P^{\rm i}/{\rm day})] = (1.1,\ 3.0,\ 0.8)$ in the plot.

surface helium abundance of the companion when $M_{\rm WD} = 1.378\,M_{\odot}$ has a strong dependence on its envelope mass (e.g., the evolution of $\dot{M}_{\rm WD}$ in Figures 4 and 19 in Meng & Podsiadlowski 2017). In Figure 4, following the definition of the core as in Han et al. (1994) and Meng et al. (2008), we show the correlation between the surface helium abundance and the envelope mass when $M_{\rm WD} = 1.378\,M_{\odot}$, where the envelope mass, $M_{\rm e}$, is defined as the difference between the companion mass, $M_2^{\rm SN}$, and the core mass, $M_{\rm c}$. The figure shows a clear anticorrelation between the envelope mass and the surface helium abundance, as expected. Therefore, the surface helium abundance may be taken as an indicator of the envelope mass at the time of supernova explosion. Similarly, Figure 3 shows that the lower the envelope mass at the time of the explosion, the more the subsequent evolutionary track will resemble the track of a hot subdwarf star (i.e., will become hotter with lower envelope mass).

2.2. The Helium Abundance and Gravity of BLAPS

As Pietrukowicz et al. (2017) showed, BLAPs are helium-rich, and their surface gravities lie between those of main-sequence stars and the known sdOB stars. If BLAPs are the surviving companions of SNe Ia, the companion predicted by the SD model will reproduce their surface helium abundance and surface gravity simultaneously. In Figure 5, we show the evolution of the surface helium abundance and surface gravity of the surviving companions, where the initial systems are the same as those in Figure 3. These figures show that, after the supernova explosion, the surviving companion from the system with $[M^{\rm i}_{\rm WD}/M_{\odot},\ M^{\rm i}_{2}/M_{\odot},\ \log(P^{\rm i}/{\rm day})] = (1.1,\ 3.0,\ 0.8)$ experiences a phase where the surface gravity decreases while the surface helium abundance increases until the star arrives on the HB. In this phase, the companion ascends the RGB, where it experiences the first dredge-up, which leads to the mixing-up of helium-rich material and an increase in the surface helium abundance. At the same time, the expansion of the star reduces the surface gravity. After the companion has settled on the HB, large-scale convection ceases in the envelope, and the surface helium abundance no longer changes. With the consumption of the envelope on the HB, the radius of the companion decreases, and the surface gravity increases until the companion becomes a BLAP (based on its position in the H-R diagram; Figure 3). This demonstrates that our surviving-companion model can simultaneously reproduce the surface helium abundance and the gravity of the BLAPs observed in Pietrukowicz et al. (2017). In particular, the surface gravity of the surviving companion in the BLAP phase lies between those of MS and hot subdwarf stars. For the star with the thinnest envelope at the time of the supernova explosion, the surface gravity during the core-helium-burning phase is higher than that of BLAPs but is consistent with sdOB stars, and the surface helium abundance and surface gravity of the companion from the system with $[M^{\rm i}_{\rm WD}/M_{\odot},\ M^{\rm i}_{2}/M_{\odot},\ \log(P^{\rm i}/{\rm day})] = (1.1,\ 3.0,\ 0.6)$ are also close to those of BLAPs, as shown in Figure 3.

2.3. The Number of BLAPs in the Galaxy

The Optical Gravitational Lensing Experiment (OGLE) project surveyed about 5% of the Milky Way disk and found 14 BLAPs (Pietrukowicz et al. 2017, private communication). At present, it is very difficult to estimate the completeness of the sample, and some BLAPs must be hidden behind clouds of dust in the surveyed directions. Here, as a very conservative upper limit, we assume that the number of BLAPs missed could be as high as 99%; this would give an estimate for the number of BLAPs in the Galaxy roughly between 280 and 28,000.

Figure 3 shows that not all surviving companions have properties consistent with those of BLAPs. To estimate the number of BLAPs from the SD model, we need to know the initial parameter space producing them. Here, we do not recalculate grids of binary evolution sequences to determine this parameter space; instead we just try to constrain it from the model grids already calculated in Meng & Podsiadlowski (2017), adopting some additional constraints. From Figures 3 and 4 we know that the envelope mass of the companion at the time of the supernova explosion is the key parameter

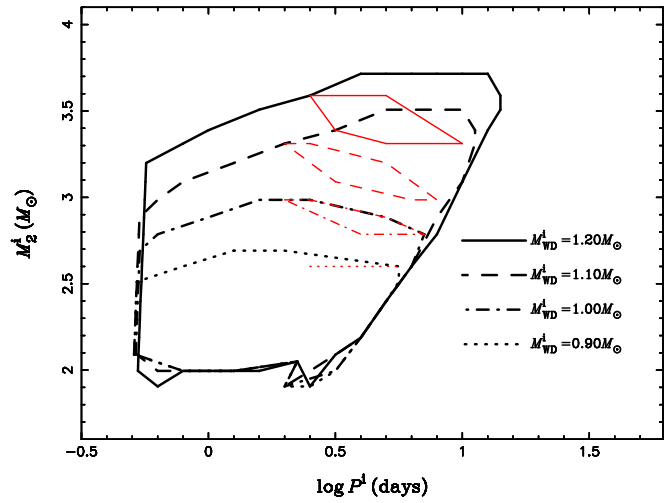

Figure 6. The initial parameter regions for different initial WD masses for BLAPs (thin red lines). For comparison, the thick lines present the parameter spaces for SNe Ia (reproduced from Meng & Podsiadlowski 2017).

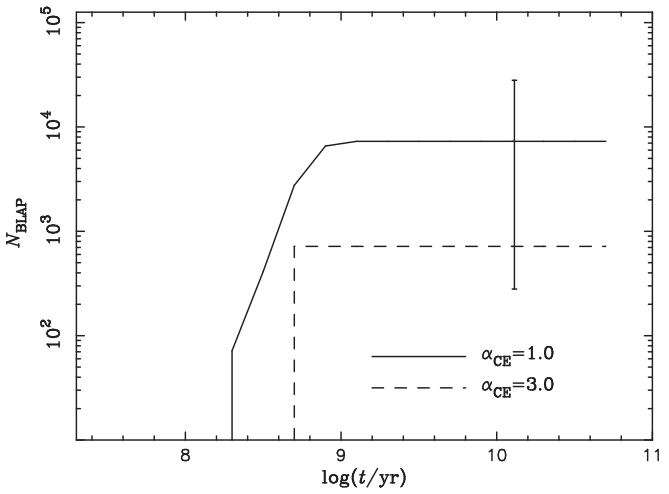

Figure 7. The evolution of the number of BLAPs in the Galaxy, where a constant star formation rate of 5 $M_\odot$ yr^{-1} is assumed. The vertical bar shows the estimated region of the number of BLAPs in the Galaxy.

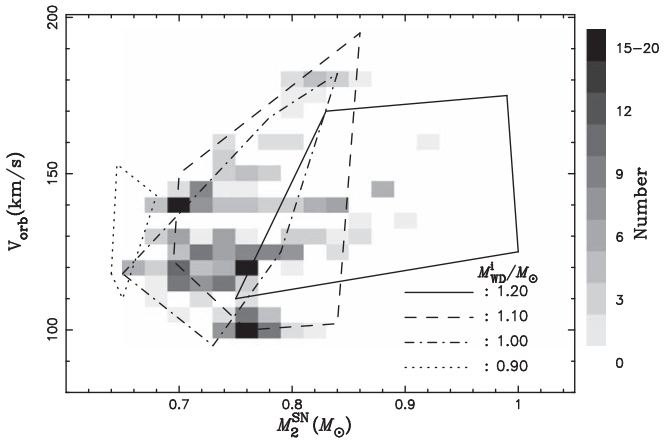

Figure 8. The distributions of companion mass and orbital velocity when $M_{\rm WD}$ = 1.378 $M_\odot$ for a constant star formation rate and $\alpha_{\rm CE}$ = 1.0. The lines present the final parameter space of the companion mass and orbital velocity for different initial WD masses.

determining whether the surviving companion produces the properties of BLAPs, and the envelope mass is anticorrelated with the surface helium abundance. Stars with a much higher or a much lower surface helium abundance produce envelopes that are either too thin or too thick and do not reproduce the location of BLAPs in the H-R diagram. As we will discuss in Section 2.5, if a star is not located in this region, it will probably not show the pulsation modes of BLAPs because of the different surface gravity or different mean density. In addition, the calculations of binary evolution in this paper do not support a companion star with a mass >1.1 $M_\odot$ at the time of the supernova explosion as a progenitor of a BLAP (the dotted line in Figures 3, see also the model simulations in Pietrukowicz et al. 2017). Considering that the observed region of BLAPs in the H-R diagram is mainly constrained by a single BLAP and that the real region could be much larger, we here assume somewhat arbitrarily that the helium abundance has to be between 0.4 and 0.6 and the companion mass less than 1.1 $M_\odot$ at the time of the explosion, so that the surviving companion can become a BLAP after central helium ignition. With these constraints, we can use the grids in Meng & Podsiadlowski (2017) to determine the parameter space that produces BLAPs; this is shown in Figure 6. This clearly shows that the initial systems that produce BLAPs consist of relatively massive WDs with massive companions and have a relatively long initial period, i.e., mass transfer begins when the companion crosses the HG. This parameter space is only a small part of the whole parameter space that leads to SNe Ia (see Figure 6), implying that the birth rate of BLAPs, ν, is much lower than the overall rate of SNe Ia from the SD model.

Based on the above parameter space, we performed two binary population synthesis (BPS) simulations using the rapid binary evolution code developed by Hurley et al. (2000, 2002), where the BPS method is the same as described in Meng & Podsiadlowski (2017). For the BPS simulations, the common-envelope ejection efficiency, $\alpha_{\rm CE}$, is the key parameter affecting the birth rate of BLAPs. Following Meng & Podsiadlowski (2017), we take $\alpha_{\rm CE}$ = 1.0 or $\alpha_{\rm CE}$ = 3.0. As the parameter space producing BLAPs is so much smaller than that producing SNe Ia, our calculations show that only 0.3% to 3.3% of all SNe Ia produce BLAPS. As shown in Figure 3, the lifetime of a BLAP is shorter than that of a typical hot subdwarf star since the progenitor of the BLAP spends part of its life in the HB phase. Simply assuming that all BLAPs have a lifetime of $\tau = 5 \times 10^7$ yr, we may obtain the evolution of the number of BLAPs with time in the Galaxy from $\nu \times \tau$, as shown in Figure 7. The predicted number of BLAPs is roughly between 750 and 7500, very much consistent with the rough estimate of BLAPs made earlier.

2.4. The Distribution of Radial Velocity

At the time of the supernova explosion, the companion in a close binary have a relatively large orbital velocity, and it will inherit this orbital velocity as runaway space velocity after the WD has been disrupted. Figure 8 shows the distributions of the orbital velocity and companion mass when $M_{\rm WD}$ = 1.378 $M_\odot$ for the systems where the companions will become BLAPs. Most of the companions have a mass of 0.76 ± 0.1 $M_\odot$ and all companions have masses below 1 $M_\odot$ although our formal adopted constraint was less than 1.1 $M_\odot$. This mass range is very much consistent with constraints from a theoretical pulsation model (~0.7–1.1 $M_\odot$, Wu & Li 2018). In addition,

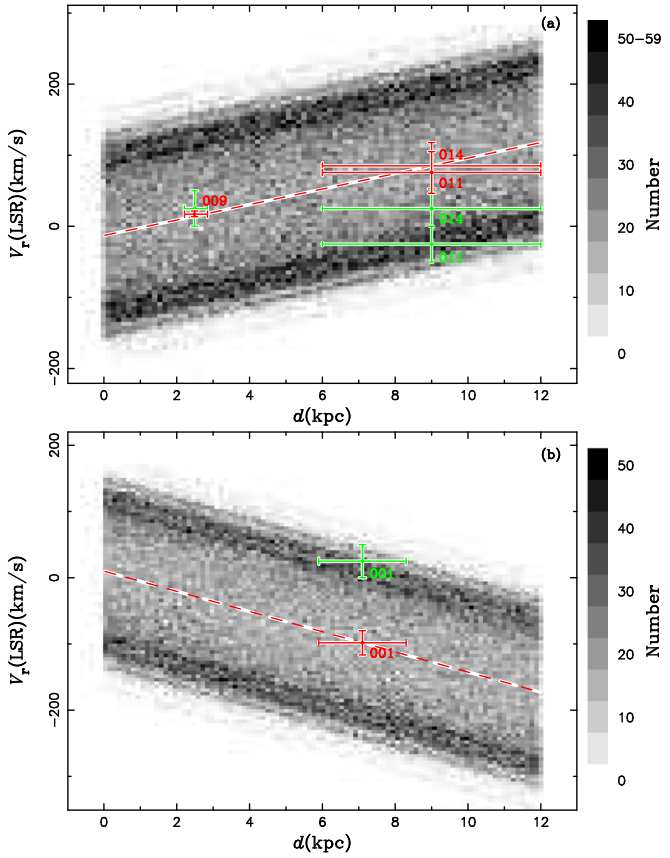

Figure 9. The distribution of the radial velocity in the local standard of rest (LSR) frame vs. distance for BLAPs, for the case $\alpha_{CE} = 1.0$. The red crosses show the positions if the observed BLAPs are disk stars, while the green crosses show the measured values (Pietrukowicz et al. 2017, private communication). The dashed lines show the correlation between radial velocity and distance in the LSR frame for disk stars, obtained from Equation (2) for the directions of (a) BLAP-014 and (b) BLAP-001.

the companion stars have space velocities between 100 and 200 km s^{-1} relative to the center of mass of the binary systems. Such a high space velocity should be reflected in the radial velocities of BLAPs.

To obtain the distribution of the radial velocity of the predicted BLAPs, we performed a Monte Carlo simulation, where the radial velocity of a surviving companion is determined by

$$V_r = V_{\rm orb} \cos i + V_{r,\rm disk}, \quad (1)$$

where i is the angle between the space velocity and the line of sight and i is generated randomly. $V_{r,\rm disk}$ is the radial velocity relative to the local standard of rest (LSR) for a disk star at a Galactic longitude l and a distance r, and is determined by

$$V_{r,\rm disk} = -V_\odot \cos(l - l_\odot) + Ar \sin(2l), \quad (2)$$

where l and $l_\odot$ are the Galactic longitudes of a disk star and the solar apex, respectively, r is the distance of the star, $V_\odot$ is the Sun's velocity in the LSR, and A is Oort's constant (Bovy 2017). Here, r is also generated in a Monte Carlo way, while l is taken to be in the directions of BLAP-014 (Figure 9(a)) and BLAP-001 (Figure 9(b)). In this discussion, we do not consider any Galactic dynamics, since the surviving companions may only travel ∼2 kpc in the Galaxy before they become BLAPs, and their positions and velocities are therefore not significantly affected by dynamical effects.

Figure 9 shows the distribution of the radial velocity of the surviving companions versus distance. The radial velocity has a larger scatter due to the different orbital velocities and inclination angle i. The distribution of the radial velocity at a given distance r has two peaks at a velocity of about $V_{r,\rm disk} \pm 110$ km s^{-1}, which is mainly caused by the different orbital velocities of the surviving companion when $M_{\rm WD} = 1.378\ M_\odot$. The correlation between $V_{r,\rm disk}$ and r is shown by two dashed lines: one corresponds to the direction of BLAP-001 and the other to the direction of BLAP-014. In the figure, we also plot the radial velocity of the BLAPs with spectral observations, where the red crosses assume that BLAPs are normal disk stars, and green crosses show the observed values (Pietrukowicz et al. 2017, private communication). Three of the four BLAPs have quite different radial velocities from disk stars in their directions and at their distances. In particular, BLAP-001 has a positive radial velocity but it should be negative if BLAP-001 were a disk star, while BLAP-011 has a negative radial velocity but it should be positive if BLAP-011 were a disk star. The differences in radial velocity between the BLAPs and the disk stars at the same position are as high as 123 ± 45 km s^{-1}. Generally, at a given distance and in a given direction, the scatter in the radial velocity of disk stars should be less than ∼20 km s^{-1} (Dehnen & Binney 1998; Anguiano et al. 2018). So, the difference in radial velocity between the BLAPs and the normal disk stars cannot be simply explained by the scatter of the radial velocity of the disk stars, and other mechanisms are required to explain it. Interestingly, the observed values of the radial velocity for BLAPs-001, 011, and 014 are located around the peak region in Figure 9. Hence, the orbital velocity could provide a reasonable explanation for the difference.

If the difference in radial velocity between the BLAPs and the disk stars mainly originates from the orbital velocity of the companion at the moment of supernova explosion, we would expect that the radial component of the orbital velocity of the companion could reproduce the difference. Here, the radial component of the orbital velocity, $|V^r_{\rm orb}|$, is set to be $|V_{\rm orb} \cos i|$, where i is again generated in a Monte Carlo way. In Figure 10, we show the distribution of the radial component of the orbital velocity of the companions for different α_{CE} and also the difference in radial velocity between the observed values and the disk stars for four BLAPs. There is a peak in the distribution, irrespective of the value of α_{CE}, consistent with those in Figure 9. Figure 10 shows that most surviving companions (∼70%–80%) have a radial velocity component between 50 and 150 km s^{-1}, while some (∼10% to 25%) have a radial component less than 50 km s^{-1}. For the four BLAPs with spectral observations, three of them have a difference in radial velocity larger than 50 km s^{-1} and one less than 50 km s^{-1}, consistent with the above distributions. We therefore conclude that our model well reproduces the difference in radial velocity between the BLAPs and the disk stars, including the distribution of the difference—key evidence in support of the surviving companion origin for BLAPs.

However, it must be emphasized that the current positions of the BLAPs in the Galaxy are not their birth sites if they are the surviving companions of SNe Ia. Based on the orbital velocity at the time of the supernova explosion and the time elapsed

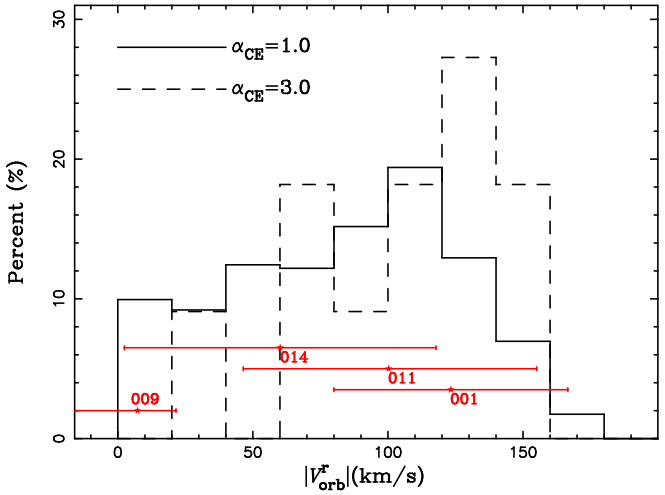

Figure 10. The distribution of the radial component of the orbital velocity of the companion when $M_{WD} = 1.378\,M_\odot$ for different α_{CE}, where a constant star formation rate is assumed. The horizontal bars show the difference in radial velocity between the observed values and the disk stars for the BLAPs with spectral observations.

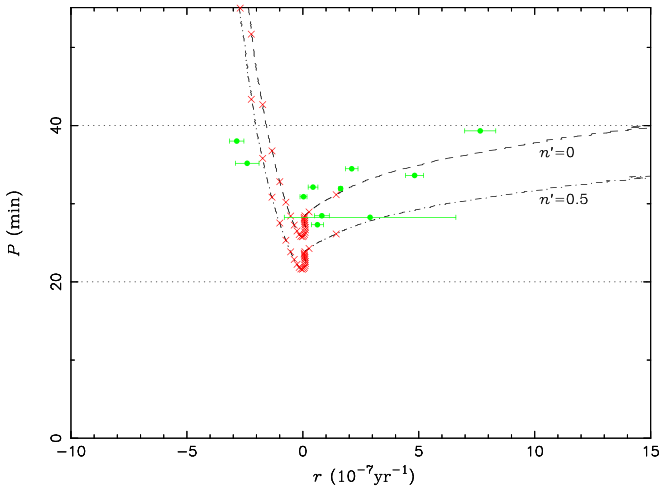

Figure 11. The evolution of the period and the rate of change in period for the model with $[M^i_{WD}/M_\odot, M^i_2/M_\odot, \log(P^i/\mathrm{day})] = (1.1, 3.0, 0.8)$ for different n'. The age interval between adjacent crosses is 10^6 yr. The green points show 11 BLAPs from Pietrukowicz et al. (2017), while the two dotted lines show the period range for the whole sample of BLAPs.

since the supernova, we estimate that they could travel ~2 kpc in the Galaxy, which adds an additional uncertainty to the difference in radial velocity of as much as 20–40 km s^{-1}. Therefore, the difference in radial velocity between the BLAPs and the normal disk stars in Figure 10 could be underestimated or overestimated by as much as 20–40 km s^{-1}. Most importantly, a significant difference in radial velocity between the BLAPs and the normal disk stars clearly exists, and the distribution of the radial component of the orbital velocity in Figure 10 can almost certainly explain this difference.

2.5. The Pulsation Period

BLAPs are mysterious variables, and at present it is completely unclear which mechanism drives their pulsations. Two processes could play an important role: one is the bump in metal opacity at $T \simeq 2 \times 10^5$ K and the other is radiative levitation of iron (Pietrukowicz et al. 2017). In Pietrukowicz et al. (2017), it is difficult to identify the pulsation mode of BLAPs based on their light curve alone, although a radial fundamental mode pulsation is favored (see also McWhirter et al. 2020). Pietrukowicz et al. (2017) presented the measured pulsation period and the rate of change in period. In our model, there is only a very thin convective zone when the companion star crosses the region of BLAPs in the H-R diagram. Therefore their pulsation modes cannot be simple, solar-type oscillations. Here, we estimate the characteristic p-mode frequency using

$$\nu_{n,l} \approx \left(n + \frac{l}{2} + \epsilon\right)\Delta\nu, \tag{3}$$

which is independent of the detailed driving mechanism (Brown et al. 1991; Kjeldse & Bedding 1995). When both radial order n and angular degree l are 0, we may obtain the frequency of the fundamental mode from

$$\nu_0 \approx \epsilon\,\Delta\nu = 134.6\epsilon\frac{(M/M_\odot)^{1/2}}{(R/R_\odot)^{3/2}}\,\mu\mathrm{Hz}, \tag{4}$$

where $\Delta\nu$ is the mean large frequency separation of a star and is calibrated to the Sun (Kjeldse & Bedding 1995; Yang & Meng 2009), and ϵ is a constant and set to 2.6 for BLAPs (Wu & Li 2018). Then, we can estimate the pulsation period as

$$P = \frac{10^6}{60}\frac{1}{(n' + \epsilon)\Delta\nu}\ \mathrm{min}, \tag{5}$$

where $n' = n + \frac{l}{2} = 0,\ 1/2,\ 1,\ 3/2,\ 2,\ldots$. Following the definition of the rate of change in period in Pietrukowicz et al. (2017), we define the rate as

$$r = \frac{\Delta P}{\Delta t}\frac{1}{P} = \frac{P_{i+1} - P_i}{t_{i+1} - t_i}\frac{1}{P_{i+1}}. \tag{6}$$

Varying n' to fit the observational data, we find that our model could reproduce the observations for $n' = 0$ or $n' = 0.5$, as shown in Figure 11. However, it is difficult to arrive at a definitive conclusion on the oscillation mode based on the results presented here. We cannot clearly distinguish between the radial fundamental mode and a nonradial p-mode oscillation. The observations of the color index of BLAPs seem to favor radial fundamental pulsations (Pietrukowicz et al. 2017). Interestingly, $n' = 0$ is the radial fundamental mode. In addition, Equation (4) shows that ν_0 is determined by the mean density of the star, i.e., stars with similar masses and similar radii will have similar ν_0. This is the reason why BLAPs have similar surface gravities and are located in similar regions in the H-R diagram. Figure 8 shows that most surviving companions have a mass around $0.76\,M_\odot \pm 0.1\,M_\odot$. When these stars cross the region of BLAPs in the H-R diagram, they will also have similar radii and similar surface gravities.

In addition, based on the results here, there is an evolutionary sequence for BLAPs with a negative and a positive rate of change in period, i.e., before stars have reached the lowest luminosity in the BLAP region, they show a negative rate of change in period, while they have a positive rate of change in period thereafter (see also Figure 3). Based on

the models in Wu & Li (2018), the sign of the rate of change in period reflects the central helium abundance of the star, Y_c, i.e., stars with $Y_c > 0.45$ show a negative rate of change in period, while those with $Y_c < 0.45$ have a positive rate of change in period, consistent with our results. It is worth emphasizing that, besides having a shorter lifetime than the observed BLAPs, the shell-hydrogen-burning model can only explain BLAPs with a negative rate of change in period (Byrne & Jeffery 2018; Córsico et al. 2018; Wu & Li 2018), while our model can produce BLAPs with both negative and positive rates simultaneously. This again suggests that BLAPs are in the middle or late core-helium-burning phase, as shown in Figure 3 (see also Wu & Li 2018). Therefore, our model naturally explains why BLAPs have similar surface gravities, similar pulsation periods, and similar rates of change in period, including their sign, at the same time. These results are not very surprising because it has previously been shown that stars in the middle or late core-helium-burning phase with a mass of $\sim$0.7 –1.1 $M_\odot$ can reproduce the pulsation properties of BLAPs (Wu & Li 2018).

3. Discussion

3.1. Metallicity

In this paper, we propose that BLAPs are the surviving companions of SNe Ia. Our model can naturally reproduce all the properties of BLAPs, including their single-star nature, their lifetime as a BLAP, their position in the H-R diagram, the surface helium abundance and gravity, the total number of BLAPs in the Galaxy, the distribution of their radial velocities, the pulsation periods, and the rate of change in period, including the sign of the rate. In addition, BLAPs are relatively young objects and are not found in low-metallicity environments (Pietrukowicz 2018). This is also a natural consequence of the dependence of the metallicity on the initial parameter space for SNe Ia. The initial parameter space in the P^i–M_2^i plane for BLAPs puts them in the upper right region for SNe Ia (see Figure 6); this means that the progenitor systems of BLAPs must contain a relatively massive companion with a relatively long orbital period. With a decrease in metallicity, it becomes more difficult for systems located in this region of parameter space to become SNe Ia. For $Z \leqslant 0.001$, no system in this region produces an SN Ia because of violent nova explosions preventing an increase in the mass of the WDs (see Figure 4 in Meng et al. 2009). Therefore the model predicts that BLAPs cannot be produced in a very low-metallicity environment, naturally explaining why BLAPs favor a young population with relatively high metallicity.

While this is based on the OTW model, we also did several binary evolution calculations with $Z = 0.001$ to test whether the above discussion still holds for our CEW model. Based on the results in Meng & Podsiadlowski (2017), we estimate that the upper boundary of the companion mass in the P^i–M_2^i plane for $Z = 0.001$ from our CEW model would be higher than that from the OTW model. We use systems with ($M_{WD}^i/M_\odot$, $M_2^i/M_\odot$) = (1.1, 2.5) but different initial periods to test the upper right boundary in the initial P^i–M_2^i plane, where the initial companion mass of 2.5 $M_\odot$ is larger than the upper-boundary mass of the initial parameter space for SNe Ia from the OTW model. The evolutionary tracks of these companions in the H-R diagram are shown in Figure 12. As expected, the upper right boundary for SNe Ia from the CEW model is higher than that from the OTW model by about 0.1 $M_\odot$, which indicates that the birth rate of SNe Ia from the CEW model is higher than that from the OTW model[6] (Meng & Podsiadlowski 2017). However, some evolutionary tracks still cross the region of BLAPs in the H-R diagram, but their lifetimes in the BLAP stage are short, and hence they are much less likely to be found as BLAPs than for $Z = 0.02$. In addition, for a star with a similar mass at the same evolutionary stage, a low metallicity implies a smaller radius (Umeda et al. 1999; Chen & Tout 2007; Meng et al. 2008), which is the main reason why the companions with $Z = 0.001$ spend most of their lives below the region of BLAPs in the H-R diagram. The smaller radius indicates that the surviving companions with $Z = 0.001$ could not show the pulsations of BLAPs (see Equation (4)) for most of their lifetimes. Moreover, the luminosity of the companions with $Z = 0.001$ in the helium-core-burning phase is generally lower than that of BLAPs, which indicates that a more massive helium core and hence a longer initial orbital period would be required to produce a BLAP. However, a system with a longer initial period, even if it is only longer by 0.1 dex, will evolve to a system of a WD + sdB star (the dotted line in Figure 12) rather than an SN Ia because of violent nova explosions and hence will not produce a BLAP.

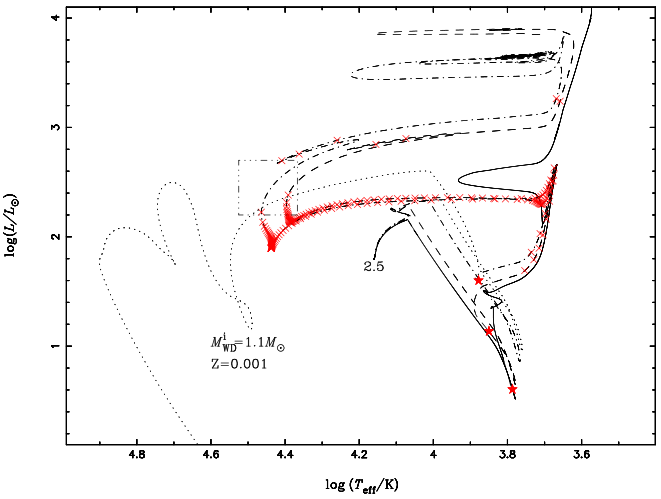

Figure 12. The evolutionary tacks of the companions for systems with $Z = 0.001$ and ($M_{WD}^i/M_\odot$, $M_2^i/M_\odot$) = (1.1, 2.5) for different initial periods, i.e. log(P^i/day) = 0.0, 0.1, 0.3, and 0.4. The red stars show the positions where the supernova explosions are assumed to occur. The age interval between adjacent crosses is 10^6 yr. The dashed–triple-dotted rectangle indicates the region of BLAPs.

The surviving companions of SNe Ia may be polluted by some heavy elements, in particular Ni and Fe, as supernova ejecta pass the companion (Marietta et al. 2000; Meng et al. 2007; Pakmor et al. 2008). Therefore, the surface abundance of such heavy elements on the surviving companions could be higher than that for typical disk stars. Enhanced heavy elements could also be helpful in producing the observed BLAP pulsations because of the increased heavy-element opacity (Pietrukowicz et al. 2017; Romero et al. 2018). However, before the companions become BLAPs, a large convective

[6] The OTW does not work when Z is lower than a certain value (e.g., $Z < 0.002$, Kobayashi et al. 1998), but the results in Meng et al. (2009) are based on the assumption that the OTW is still valid for low metallicities. If the metallicity constraint is considered (e.g., $Z = 0.001$), the upper right boundary of the parameter space for SNe Ia and the birth rate of SNe Ia from the CEW model are probably significantly higher than those from the OTW model.

region is likely develop in the envelope, mixing such heavy elements from the supernova ejecta into the interior and making such anomalies unobservable. At the same time, at high effective temperature, radiative levitation effects could bring the inner iron-group elements to the surface of the star in the BLAP stage, as observed in the spectra of some subdwarf O stars (Chayer et al. 1995; Charpinet et al. 1997; Latour et al. 2018). Generally, the timescales for the above two effects are much shorter than the typical evolutionary timescale of hot subdwarf stars (Dorman et al. 1993; Charpinet et al. 1997); hence BLAPs are likely to have lost the information on the chemical pattern due to any pollution by supernova ejecta. In any case, with currently only moderate-resolution spectra available, the abundance of the heavy elements cannot be determined. Even if higher abundances were to be determined by future observations, this would not constitute key evidence in support of the surviving-companion nature of BLAPs.

If the initial metallicity of the progenitor system were not to affect the production of BLAPs, we would expect about 10–100 BLAPs in the Large Magellanic Cloud (LMC), based on the birth rate of BLAPs in the Galaxy and the star formation history in the LMC (Harris & Zaritsky 2009). However, no BLAPs have so far been observed in the LMC and SMC (Pietrukowicz 2018). This indicates that the initial metallicity plays an important role in the production of BLAPs, probably by affecting the parameter space for SNe Ia, as discussed above based on the SD model for SNe Ia. In addition, radiative levitation is probably required to produce the pulsation modes of BLAPs, and an enhancement of iron and nickel could be a key factor in the development of the pulsations seen in BLAPs (Jeffery & Saio 2016; Byrne & Jeffery 2018; Romero et al. 2018). Our surviving companion scenario for BLAPs provides a natural explanation for the enhancement of iron and nickel by the pollution from supernova ejecta.

3.2. Uncertainties

In this paper, we assumed that a CO WD explodes as an SN Ia when $M_{\rm WD} = 1.378\,M_{\odot}$. We then followed the evolution of the companion star and found that some companions can reproduce the properties of BLAPs. However, there are two other effects that could influence the companions and change the initial parameter space producing BLAPs. One is the collision of supernova ejecta with the companions (Marietta et al. 2000; Meng et al. 2007; Pakmor et al. 2008; Liu et al. 2012), the other is the so-called spin-up/spin-down model (Justham 2011; Di Stefano & Kilic 2012).

For the SD model, the supernova ejecta may collide with the envelope of the companion and strip off part of the envelope. The amount of material stripped off is heavily dependent on the structure of the companion (Meng et al. 2007; Pakmor et al. 2008). For the systems leading to BLAPs, the impact of the supernova ejecta may strip off about $0.065\,M_{\odot}$ to $0.125\,M_{\odot}$ from the surface of the companion, mainly depending on the ratio of the binary separation to the companion radius at the moment of supernova explosion (Meng et al. 2007; Liu et al. 2012; Pan et al. 2012). The stripped hydrogen-rich material may reveal itself by a narrow Hα emission line in the late-time spectrum (Marietta et al. 2000; Meng et al. 2007). However, such a prediction was not confirmed by the observations of most SNe Ia (Maguire et al. 2016; Tucker et al. 2020). On the other hand, the narrow Hα emission line was indeed detected in some SNe Ia, but the amount of hydrogen-rich material deduced from observations is much smaller than the theoretical predictions (Maguire et al. 2016; Prieto et al. 2020). At present, the reason for the conflict between observation and theory is still unclear.

After the impact, the companion may be heated and may expand quickly to a luminosity as high as a few $10^3\,L_{\odot}$, and the energy deposited in the envelope of the companion will take a thermal timescale to release (Marietta et al. 2000; Podsiadlowski 2003; Shappee et al. 2013; Pan et al. 2014). Then, during this period, the companion may introduce an extra stellar wind, reducing the envelope mass further. However, assuming a simple Reimer's wind and taking typical values of the luminosity ($10^3\,L_{\odot}$), the radius ($10^2\,R_{\odot}$), and the thermal timescale (10^4 yr) of the companion (Shappee et al. 2013), the companion would lose about $10^{-4}\,M_{\odot}$ during this period. Therefore, such an effect can be neglected.

The WDs in the systems may spin up as they gain angular momentum from the accreted material. Rapidly rotating WDs, however, may exceed the classical Chandrasekhar mass limit, and rotating super-Chandrasekhar WDs require a spin-down phase before they can explode as SNe Ia (Justham 2011; Di Stefano & Kilic 2012). The spin-down timescale is currently quite uncertain, probably between 10^5 yr and 10^7 yr (Di Stefano et al. 2011; Meng & Podsiadlowski 2013). Based on the CE mass and the mass-loss rate at the moment when $M_{\rm WD} = 1.378\,M_{\odot}$, Meng & Podsiadlowski (2018) estimated that a spin-down timescale of $\sim 10^6$ yr is favored. During the spin-down phase, the companion may continue to lose envelope material. However, since the companion only has a very thin envelope, the mass-loss rate would decrease quickly to less than $10^{-7}\,M_{\odot}$ yr^{-1}, even stopping completely (this is the main reason why the OTW model cannot produce SNe Ia in the upper right region of the initial parameter space, while the CEW can; see Figure 2 and the detailed discussions in Meng et al. 2009). The companion may not lose too much material during the spin-down phase, i.e., probably less than $0.1\,M_{\odot}$.

Therefore, the effects discussed above on the mass of the companion are similar, i.e., a decrease in its mass at the time of the supernova explosion. This could make the companions more similar to hot subdwarf stars rather than BLAPs when helium is ignited in the center, as the model with $[M^{\rm i}_{\rm WD}, M^{\rm i}_2/M_{\odot}, \log(P^{\rm i}/{\rm day})] = (1.1, 3.3, 0.9)$ shows. In this case, models such as $[M^{\rm i}_{\rm WD}, M^{\rm i}_2/M_{\odot}, \log(P^{\rm i}/{\rm day})] = (1.1, 3.0, 0.6)$ would become the progenitors of BLAPs. Therefore, the main consequence of these effects would be to change the initial parameter space producing BLAPs, i.e., the initial parameter space moves to shorter initial period in Figure 6. Hence, the predicted number of BLAPs here could be underestimated or overestimated (see Figure 11 in Meng et al. 2009). However, at present, the number of BLAPs in our Galaxy is quite uncertain, and even if the uncertainty of the theoretically predicted number is as high as 100%, the number of BLAPs predicted here is still consistent with the present observational constraint. Therefore, the effects discussed above would not significantly affect our main conclusions.

Besides the influence on the companion mass, these two effects might also change the space velocity of the surviving companions but in opposite directions. Compared with the orbital velocity when $M_{\rm WD} = 1.378\,M_{\odot}$, the collision of supernova ejecta with the companion increases its space velocity because it imparts a kick, but the kick velocity would be significantly smaller than the orbital velocity (Marietta et al. 2000;

Meng et al. 2007; Meng & Podsiadlowski 2017). In contrast, a spin-down phase may significantly decrease the orbital velocity. For example, if a spin-down timescale of a few 10^6 yr is considered, the orbital velocity of the companion at the time of the supernova explosion would be in the range 50–190 km s^{-1} (Meng & Li 2019). Therefore, the effect of the spin-down mechanism is likely to dominate in determining the final space velocity of the surviving companions. On both the observational and theoretical sides, a spin-down phase seems likely to be necessary (Soker 2017; Meng & Podsiadlowski 2018), which means a smaller space velocity for the surviving companions of SNe Ia than that shown in Figure 8. Therefore, the proportion of systems with radial velocity less than 50 km s^{-1} in Figure 10 is likely to be underestimated.

The Gaia project provides a unique opportunity to constrain the origin of BLAPs. However, for the 14 BLAPs in Pietrukowicz et al. (2017), only BLAP-009 has a reliable parallax measurement in Gaia DR2. Based on the proper motion and distance from Gaia DR2 data and the radial velocity in Figure 9, we can obtain the components of the space velocity of BLAP-009 in the Milky Way's Galactic coordinate system: $U = 39.8 \pm 35.1$ km s^{-1}, $V = 182.9 \pm 13.4$ km s^{-1}, and $W = 13.4 \pm 2.5$ km s^{-1} (Astraatmadja & Bailer-Jones 2016; Luri et al. 2018). Hence, BLAP-009 has a lower space velocity than a typical disk star around its location by $\sim 60 \pm 22$ km s^{-1}, i.e., BLAP-009 may even be taken as a runaway star, considering the large difference in space velocity (Blaauw 1961; Brown 2015; Huang et al. 2016). The velocity difference of 60 ± 22 km s^{-1} is smaller than the prediction in Figure 8, but is consistent with the results in Meng & Li (2019), which would imply that a spin-down phase is necessary for the production of BLAPs if they are the surviving companions of SNe Ia.[7]

The measurement of the masses of BLAPs could provide a key clue to constrain their origin, but unfortunately there are too many uncertainties to estimate the masses of the BLAPs—uncertainties in their distances, brightnesses, surface gravities, and effective temperatures. If all these uncertainties are considered, the mass of BLAP-009 could be anywhere between 0.06 $M_\odot$ and 1.40 $M_\odot$, hence providing no meaningful constraint.

3.3. Other Possible Origins

As discussed in Pietrukowicz et al. (2017), BLAPs are core-helium-burning or hydrogen-shell-burning stars with thin envelopes. For the hydrogen-shell-burning model, BLAPs are possibly the progenitors of extremely low-mass WDs with high effective temperatures and a stellar mass of $\sim 0.34\,M_\odot$[8] (Romero et al. 2018). But the lifetime of the hydrogen-shell-burning stars in the BLAP stage is too short to be compatible with the long-term stability of the pulsation periods of observed BLAPs with a typical timescale of 10^7 yr (Podsiadlowski et al. 2002; Wu & Li 2018). Even if the progenitors of extremely low-mass WDs were to contribute to the BLAP population, they could only produce BLAPs with a negative rate of change in period (Byrne & Jeffery 2018; Córsico et al. 2018; Wu & Li 2018). Therefore, the core-helium-burning model is the favored model for BLAPs, as predicted by our model. Nevertheless, there are potentially several other channels to form such a structure. However, as discussed in the following, no other channel currently considered can explain all the properties of BLAPs simultaneously, and every alternative channel has its problems. As we will show now, only the surviving companion scenario may be able to solve all problems simultaneously.

To form the structure of a BLAP, a star needs to lose its envelope in the HG or on the first giant branch (FGB). Since BLAPs are single stars, single-star channels need to be considered. For a single star with $M_i \leqslant 1.0\,M_\odot$ and metallicity $Z \geqslant 0.02$, a star may lose most or all of its envelope near the tip of the FGB because these envelopes are extremely weakly bound (Han et al. 1994; Meng et al. 2008). If a thin envelope remains and helium is ignited in the center of the remnant after envelope ejection, the star would show the main properties of BLAPs. Such a channel could easily explain the dependence of the BLAPs on metallicity. However, BLAPs from such a channel would belong to an old population, which is inconsistent with their young-population nature. In addition, this origin would not explain the unusual radial velocity of BLAPs. If this channel contributes to BLAPs, there should be many in old metal-rich clusters, e.g., NGC 6791, but no BLAPs have been reported in NGC 6791. Also, if helium is ignited in the center after envelope ejection, the star is more likely to become a hot subdwarf star than a BLAP (Kalirai et al. 2007; Steinfadt et al. 2012; Han & Chen 2013).

Another possible channel to form the structure of a BLAP is also from the SD scenario for SNe Ia, where the companion of the WD is a red giant star, i.e., comes from the WD + RG channel. After the supernova explosion, the supernova ejecta may strip off almost all the envelope of the RG companion (Marietta et al. 2000). If the hydrogen shell is still burning, the companion could show the properties of BLAPs (e.g., the shell-hydrogen-burning model in Pietrukowicz et al. 2017). However, this channel also has problems with the population and radial velocity as discussed above (Wang et al. 2010). In addition, the envelope of the companion after the collision with the supernova ejecta is so thin (i.e., less than 0.02 $M_\odot$) that the lifetime of the companion in the shell-burning stage is too short (i.e., shorter than 10^5 yr) to explain the long-term stability of the pulsation periods of BLAPs with a typical timescale of 10^7 yr. After the extinction of the hydrogen shell, helium generally cannot be ignited in the center of the star because of its low mass, and the companion probably becomes a low-mass single WD rather than a BLAP (Justham et al. 2009; Meng & Yang 2010; Meng & Han 2016). Even if helium were ignited in the center, the companion would appear as a hot subdwarf with a mass of less than 0.45 $M_\odot$ rather than a BLAP (Meng & Podsiadlowski 2013).

Pietrukowicz et al. (2017) discussed a possible origin from the Galactic Center, i.e., the progenitors of BLAPs would be members of binary systems passing the central supermassive black hole, where the companions are captured by the supermassive black hole while the progenitors of the BLAPs are ejected from the Galactic Center. However, the position of BLAPs in the Galaxy and their radial velocities do not support such a runaway scenario. The conclusive evidence to exclude

[7] Although the distances of other BLAPs are not as precise as for BLAP-009 in Gaia DR2, we show the components of the space velocity of BLAP-014—the distance of which is relatively precise compared to other BLAPs—in the Milky Way's Galactic coordinate system as a reference, i.e., $U = 35.6 \pm 34.9$ km s^{-1}, $V = 159.6 \pm 61.4$ km s^{-1}, and $W = -11.9 \pm 11.7$ km s^{-1}. Therefore, BLAP-014 has a lower space velocity than a typical disk star around its location by $\sim 79 \pm 62$ km s^{-1}.

[8] Recently, Kupfer et al. (2019) found a new class of BLAPs with higher surface gravities and proposed that this new class are extremely low-mass WDs. We will address this class in another paper.

the runaway scenario comes from the Gaia observation for BLAP-009, as discussed in Section 3.2. The components of the space velocity of BLAP-009 in the Milky Way's Galactic coordinate system and its distance of 5.50 ± 0.53 kpc from the Galactic Centre clearly prove that it cannot originate from there.

Since BLAPs could be related to hot subdwarfs, another channel to form single hot subdwarf stars could also contribute to BLAPs, i.e., if the progenitor of a BLAP is an FGB star in a binary system. If the companion of the FGB is a low-mass star or a brown dwarf, possibly even as small as a planet, the system could merge during a CE phase and form a rapidly rotating HB star. The centrifugal force for rapid rotation may enhance the mass loss from the surface of the HB star and a BLAP might form (Soker 1998; Politano et al. 2008). This scenario could easily explain why BLAPs seem to be connected with hot subdwarf stars, but it is difficult to explain the distribution of their radial velocities and their young-population nature. Similarly, the merger of two helium WDs to form a single hot subdwarf star also does not explain the metallicity dependence and the unusual radial velocities. Moreover, the merger scenario of two helium WDs is expected to produce extremely hydrogen-deficient hot subdwarf stars, inconsistent with BLAPs (Zhang & Jeffery 2012).

Pietrukowicz et al. (2017) could not exclude the possibility that some BLAPs have very faint companions. So, subdwarf stars in long-period binary systems could contribute to the BLAP population (Han et al. 2002, 2003; Chen et al. 2013). However, such a channel has the same problems as the previous models with the metallicity dependence and radial velocity distribution of BLAPs.

There is another puzzle for channels related to the formation of normal hot subdwarf stars: why have BLAPs only been discovered recently, unlike hot subdwarf stars. The most reasonable explanation is that the formation process for BLAPs is not associated with the normal hot subdwarf channel, and that the number of BLAPs is much smaller than that of normal hot subdwarf stars. Based on the results in this paper and Han et al. (2003), we may estimate that the theoretical ratio of the number of single hot subdwarf stars to BLAPs lies roughly between 6 and 640. Currently, about 2000 hot subdwarf stars have been confirmed spectroscopically, but the single-star frequency among them is still uncertain (Geier et al. 2015, 2017; Kepler et al. 2015, 2016; Luo et al. 2016). It probably lies between 10% and 50% (see the discussion in Han et al. 2003). So, the number of discovered single hot subdwarfs lies roughly between 200 and 1000; this would imply that the observational number ratio of single hot subdwarf stars to BLAPs is between 14 and 71, consistent with our theoretical estimates. When the total catalog of hot subdwarf stars before the Gaia mission is considered, the ratio may increase up to 200, still in the range of the theoretical estimates (Geier et al. 2017). Therefore, the theoretical and the observed number ratios appear consistent with each other, at least at the present observational level.

Our model makes a prediction of the distribution of BLAPs in the Galaxy. The progenitors are born in the thin disk and then spread in all directions. Since there is continuous star formation in the thin disk, we may expect that the number density of BLAPs is highest in the thin disk, lower in the thick disk, and lowest in the halo. Future surveys may be able to check this prediction.

3.4. A New Channel to Form Single Hot Subdwarf Stars

As we showed in this paper, some systems from the same channel that produces BLAPs but with slightly different initial parameters can produce single hot subdwarf stars (see Figure 3). This is in fact a new channel to form single hot subdwarf stars, which may have different properties from those forming from other, more canonical evolutionary scenarios, e.g., (a) the merger of two helium WDs, (b) the merger of an FGB star and its low-mass companion, and (c) the envelope ejection scenario for single low-mass high-metallicity FGB stars (see the discussions in the above section and Han et al. 1994, 2002, 2003; Heber 2009; Meng et al. 2008).

(1) Generally, hot subdwarf stars from scenario (a) are extremely helium-rich sdOs with strong N lines in their atmospheres (Heber 2009; Zhang & Jeffery 2012). These extremely helium-rich sdOs usually have $\log(n_{\rm He}/n_{\rm H})$ larger than 0, even larger than 1 (Luo et al. 2016), while the single hot subdwarf stars from scenarios (b) and (c) usually have $\log(n_{\rm He}/n_{\rm H})$ less than -1. However, the single hot subdwarf stars from our model generally have a medium $\log(n_{\rm He}/n_{\rm H})$ value, i.e., between 0 and -1 (see Figure 5).
(2) The mass of the single subdwarf stars from scenarios (a), (b), and (c) has a broad range from 0.3 to $0.8\,M_{\odot}$ and peaks at the canonical mass for the He core-flash at $0.46\,M_{\odot}$ (Han et al. 2003; Meng et al. 2008; Politano et al. 2008; Han & Chen 2013), while the single hot subdwarf stars from our model have a mass larger than $0.5\,M_{\odot}$, up to $0.97\,M_{\odot}$ (Meng & Podsiadlowski 2017).
(3) The present sample of single hot subdwarf stars are mainly found in the thick disk or halo of the Galaxy, which means that they belong to a relatively old population (Luo et al. 2016), while the hot subdwarf stars from our model belong to a young population and could be found in the thin or thick disk of the Galaxy.
(4) The hot subdwarf stars from our model inherit the orbital velocities of the binary systems at the time of the supernova explosion and will show a different space velocity to those from scenarios (a), (b), and (c). In addition, Figures 2 and 6 show that the OTW model has difficulties in producing such single hot subdwarf stars. Hence, the discovery of such hot subdwarf stars will favor our CEW model.

Interestingly, there exists a small group in the current sample of hot subdwarf stars, consistent with our predictions but difficult to explain by standard binary evolutionary channels (e.g., group 4 in Figure 8 of Luo et al. 2016). Figure 13 shows the evolution of the surface helium abundance and the effective temperature of the companions from the systems with $[M^{\rm i}_{\rm WD}/M_{\odot}, M^{\rm i}_{2}/M_{\odot}, \log(P^{\rm i}/{\rm day})] = (1.1, 3.3, 0.9)$. The figure shows that the companion after the supernova explosion spends most of its life in the region of group 4 in Luo et al. (2016); hence our model provides a reasonable origin for this group. Also, the figure shows that, if the spin-down timescale is as long as 6 Myr, the companion star could become a hot subdwarf star before the supernova explosion (Meng & Li 2019). Such a spin-down timescale of a rapidly rotating WD is consistent with the estimate in Meng & Podsiadlowski (2013). This result could open a new window for searching for a surviving companion in a supernova remnant or the progenitor system in archival images taken before the

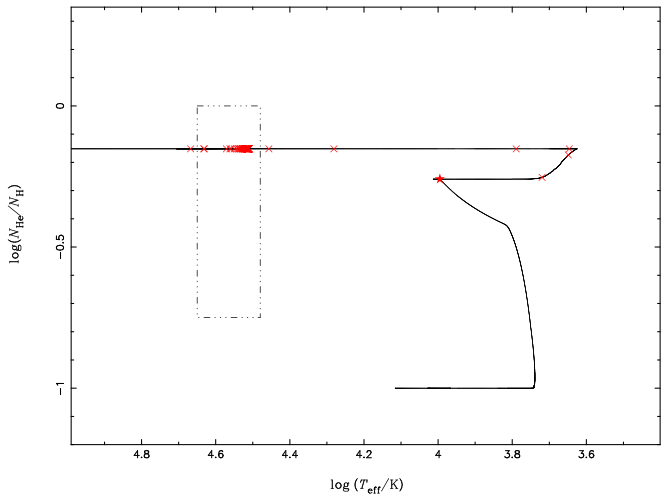

Figure 13. The evolution of the surface helium abundance and effective temperature for the model with $[M^i_{WD}/M_\odot, M^i_2/M_\odot, \log(P^i/\mathrm{day})] = (1.1, 3.3, 0.9)$. The dashed–triple-dotted rectangle shows the region for group 4 of hot subdwarf stars in Luo et al. (2016, private communication). Red stars show the position where supernova explosions are assumed to occur, and the age interval between adjacent crosses is 10^6 yr.

supernova explosion (Meng & Li 2019). However, the properties of the hot subdwarf stars from our SN Ia channel could be difficult to distinguish from those originating from the CE merger channel, except that the atmosphere of the hot subdwarf stars from the SNe Ia channel could be polluted by supernova ejecta. However, the heavy elements from such pollution would not be a good tracer to distinguish different origins, as discussed in Section 3.1. One possible mechanism to distinguish the hot subdwarf stars from these two channels is to measure their radial velocity since the radial velocity of the stars from the SN Ia channel is generally larger than that from other channels. Moreover, the distribution of such single hot subdwarf stars in the Galaxy provides another clue to distinguish them from other single hot subdwarf stars since they are mainly located in the thin disk and few should be found in the halo, similar to BLAPs. We will investigate this channel in more detail in the future.

4. Conclusion

In summary, we propose that the mysterious BLAPs are the surviving companions of SNe Ia, since all the properties of the BLAPs may be reasonably reproduced by our SD model simultaneously, including their population characteristics, positions in the H-R diagram, spectroscopic properties, radial velocities, pulsation periods and their rates of change in period, and the total number of BLAPs in the Galaxy. No other proposed channel can simultaneously explain all these properties. We predict the distribution of BLAPs in the Galaxy, with their number density being highest in the thin disk, lower in the thick disk, and lowest in the halo. We also predict a new channel for *single* hot subdwarf stars, which connects them directly to BLAPs with a generally high radial velocity. Such single hot subdwarf stars have a similar space distribution to BLAPs in the Galaxy. If such hot subdwarf stars are confirmed observationally, this would provide additional support for our CEW model. Interestingly, there already exists a small group of objects in the currently known sample of single hot subdwarf stars with properties consistent with our model predictions.

We are grateful to Pawel Pietrukowicz, Yan Li, and Tao Wu for their kind help and discussions. This work was supported by the NSFC (Nos. 11973080, 11521303, and 11733008). X.M. acknowledges the support by the Yunnan Ten Thousand Talents Plan Young & Elite Talents Project.

ORCID iDs

Xiang-Cun Meng https://orcid.org/0000-0001-5316-2298
Zhan-Wen Han https://orcid.org/0000-0001-9204-7778

References

Anguiano, B., Majewski, S. R., Freeman, K. C., Mitschang, A. W., & Smith, M. C. 2018, MNRAS, 474, 854
Astraatmadja, T. L., & Bailer-Jones, C. A. L. 2016, ApJ, 832, 137
Blaauw, A. 1961, BAN, 15, 265
Bovy, J. 2017, MNRAS, 468, L63
Branch, D. 2004, Natur, 431, 1044
Brown, T. M., Gilliland, R. L., Noyes, R. W., & Ramsey, L. W. 1991, ApJ, 368, 599
Brown, W. R. 2015, ARA&A, 53, 15
Byrne, C. M., & Jeffery, C. S. 2018, MNRAS, 481, 3810
Charpinet, S., Fontaine, G., Brassard, P., et al. 1997, ApJ, 483, L123
Chayer, P., Fontaine, G., & Wesemael, F. 1995, ApJS, 99, 189
Chen, X., Han, Z., Deca, J., & Podsiadlowski, Ph. 2013, MNRAS, 434, 186
Chen, X., & Tout, C. A. 2007, ChJAA, 7, 245
Córsico, A. H., Romero, A. D., Althaus, L. G., Pelisoli, I., & Kepler, S. O. 2018, arXiv:1809.07451
Dehnen, W., & Binney, J. J. 1998, MNRAS, 298, 387
Di Stefano, R., & Kilic, M. 2012, ApJ, 759, 56
Di Stefano, R., Voss, R., & Claeys, J. S. W. 2011, ApJL, 738, L1
Dorman, B., Rood, R. T., & O'Connell, R. W. 1993, ApJ, 419, 596
Geier, S., Kupfer, T., Heber, U., et al. 2015, A&A, 577, A26
Geier, S., Østensen, R. H., Nemeth, P., et al. 2017, A&A, 600, 50
Hachisu, I., Kato, M., & Nomoto, K. 1996, ApJL, 470, L97
Han, Z. 2008, ApJL, 677, L109
Han, Z., & Chen, X. 2013, in 40th Liège International Astrophysical Colloquium. Ageing Low Mass Stars: From Red Giants to White Dwarfs, 43 (Liège: EPJ Web of Conferences), 01007
Han, Z., Podsiadlowski, P., & Eggleton, P. P. 1994, MNRAS, 270, 121
Han, Z., Podsiadlowski, Ph., Maxted, P. F. L., & Marsh, T. R. 2003, MNRAS, 341, 669
Han, Z., Podsiadlowski, Ph., Maxted, P. F. L., Marsh, T. R., & Ivanova, N. 2002, MNRAS, 336, 449
Harris, J., & Zaritsky, D. 2009, AJ, 138, 1243
Heber, U. 2009, ARA&A, 2009, 211
Hillebrandt, W., & Niemeyer, J. C. 2000, ARA&A, 38, 191
Howell, D. A. 2011, NatCo, 2E, 350
Hoyle, F., & Fowler, W. A. 1960, ApJ, 132, 565
Huang, Y., Liu, X. W., Yuan, H. B., et al. 2016, MNRAS, 463, 2623
Hurley, J. R., Pols, O. R., & Tout, C. A. 2000, MNRAS, 315, 543
Hurley, J. R., Tout, C. A., & Pols, O. R. 2002, MNRAS, 329, 897
Iben, I., & Tutukov, A. V. 1984, ApJS, 54, 335
Jeffery, C. S., & Saio, H. 2016, MNRAS, 458, 1352
Justham, S. 2011, ApJL, 730, L34
Justham, S., Wolf, C., Podsiadlowski, P., & Han, Z. 2009, A&A, 493, 1081
Kalirai, J. S., Bergeron, P., Hansen, B. M. S., et al. 2007, ApJ, 671, 748
Kepler, S. O., Pelisoli, I., Koester, D., et al. 2015, MNRAS, 446, 4078
Kepler, S. O., Pelisoli, I., Koester, D., et al. 2016, MNRAS, 455, 3413
Kjeldse, H., & Bedding, T. R. 1995, A&A, 293, 87
Kobayashi, C., Tsujimoto, T., Nomoto, K., et al. 1998, ApJL, 503, L155
Kupfer, Th., Bauer, E. B., Burdge, K. B., et al. 2019, ApJL, 878, L35
Latour, M., Chayer, P., Green, E. M., Irrgang, A., & Fontaine, G. 2018, A&A, 609, A89
Li, C., Chu, Y., Gruendl, R. A., et al. 2017, ApJ, 836, 85
Liu, Z. W., Pakmor, R., Röpke, F. K., et al. 2012, A&A, 548, A2
Luo, Y., Németh, P., Liu, C., Deng, L., & Han, Z. 2016, ApJ, 818, 202
Luri, X., Brown, A. G. A., Sarro, L. M., et al. 2018, A&A, 616, A9
Maguire, K., Taubenberger, S., Sullivan, M., & Mazzali, P. A. 2016, MNRAS, 457, 3254
Maoz, D., Mannucci, F., & Nelemans, G. 2014, ARA&A, 52, 107
Marietta, E., Burrows, A., & Fryxell, B. 2000, ApJS, 128, 615
McWhirter, P. R., Lam, M. C., & Steele, I. A. 2020, MNRAS, 496, 1105

Meng, X., Chen, X., & Han, Z. 2007, PASJ, 59, 835
Meng, X., Chen, X., & Han, Z. 2008, A&A, 487, 625
Meng, X., Chen, X., & Han, Z. 2009, MNRAS, 395, 2103
Meng, X., Gao, Y., & Han, Z. 2015, IJMPD, 24, 1530029
Meng, X., & Han, Z. 2016, A&A, 588, A88
Meng, X., & Li, J. 2019, MNRAS, 482, 5651
Meng, X., & Podsiadlowski, P. H. 2013, ApJL, 778, L35
Meng, X., & Podsiadlowski, P. H. 2017, MNRAS, 469, 4763
Meng, X., & Podsiadlowski, P. H. 2018, ApJ, 861, 127
Meng, X., & Yang, W. 2010, A&A, 516, A47
Nomoto, K., Thielemann, F-K., & Yokoi, K. 1984, ApJ, 286, 644
Pakmor, R., Röopke, F. K., Weiss, A., & Hillebrandt, W. 2008, A&A, 489, 943
Pan, K., Ricker, P. M., & Taam, R. E. 2012, ApJ, 750, 151
Pan, K., Ricker, P. M., & Taam, R. E. 2014, ApJ, 792, 71
Perlmutter, S., Aldering, G., Goldhaber, G., et al. 1999, ApJ, 517, 565
Pietrukowicz, P. 2018, in The RR Lyrae 2017 Conference. Revival of the Classical Pulsators: from Galactic Structure to Stellar Interior Diagnostics., Vol. 6., ed. R. Smolec, K. Kinemuchi, & R. I. Anderson (Poland: Proc. Polish Astronomical Soc.), 258
Pietrukowicz, P., Dziembowski, W. A., Latour, M., et al. 2017, NatAs, 1E, 166
Podsiadlowski, P. H. 2003, arXiv:astro-ph/0303660
Podsiadlowski, Ph., Rappaport, S., & Pfahl, E. D. 2002, ApJ, 565, 1107
Politano, M., Taam, R. E., van der Sluys, M., & Willems, B. 2008, ApJL, 687, L99
Prieto, J. L., Chen, P., Dong, S., et al. 2020, ApJ, 889, 100
Riess, A., Filippenko, A. V., Challis, P., et al. 1998, AJ, 116, 1009
Romero, A. D., Córsico, A. H., Althaus, L. G., Pelisoli, I., & Kepler, S. O. 2018, MNRAS, 477, L30
Ruiz-Lapuentec, P., Comeron, F., Méndez, J., et al. 2004, Natur, 431, 1069
Sarbadhicaryc, S. K., Badenes, C., Chomiuk, L., et al. 2017, MNRAS, 464, 2326
Shappee, B. J., Kochanek, C. S., & Stanek, K. Z. 2013, ApJ, 765, 150
Shen, K. J., Boubert, D., Gänsicke, B. T., et al. 2018, ApJ, 865, 15
Soker, N. 1998, AJ, 116, 1308
Soker, N. 2017, SCPMA, 61, 049502
Steinfadt, J. D. R., Bildsten, L., Kaplan, D. L., et al. 2012, PASP, 124, 1
Tucker, M. A., Shappee, B. J., Vallely, P. J., et al. 2020, MNRAS, 493, 1044
Umeda, H., Nomoto, K., Yamaoka, H., et al. 1999, ApJ, 513, 861
Wang, B., & Han, Z. 2012, NewAR, 56, 122
Wang, B., Li, X., & Han, Z. 2010, MNRAS, 401, 2729
Webbink, R. F. 1984, ApJ, 277, 355
Whelan, J., & Iben, I. 1973, ApJ, 186, 1007
Wu, T., & Li, Y. 2018, MNRAS, 478, 3871
Yang, W., & Meng, X. 2009, PASJ, 61, 1399
Zhang, X., & Jeffery, C. S. 2012, MNRAS, 419, 452